

Solution Processed Zinc Indium Tin Oxide Thin Films for Thin Film Transistor Applications

A thesis submitted
in partial fulfillment of the requirements for
the award of degree of

MASTER OF PHYSICS
at
Thapar University, Patiala

Submitted by
NIDHI
Roll No.301404015

Under the guidance of
Dr. Bhaskar Chandra Mohanty
Associate Professor
School of Physics and Materials Science
Thapar University, Patiala



SCHOOL OF PHYSICS AND MATERIALS SCIENCE

Thapar University

Patiala -147004, India

CERTIFICATE

I hereby declare that the project work is an authentic record of our work carried out at Thapar University, Patiala as required for six months project semester for the award of degree of **M.Sc Physics** from Thapar University, Patiala, under the guidance of Dr. B.C. Mohanty for the period of six months i.e. from January 2016 to June 2016.

Date: July 15, 2016

Nidhi
Nidhi
301404015

Certified that the above statement made by the student is correct to the best of my knowledge and belief.



(Dr. B. C. Mohanty)
Associate Professor
School of Physics and Material Science
Thapar University, Patiala-147004 (Punjab)



(Dr. Manoj Kumar Sharma)
Professor & Head
School of Physics and Material Science
Patiala -147004 (Punjab)

S. S. Bhatia
Dr. S. S. Bhatia
Dean of Academic Affairs
Thapar University, Patiala

DECLARATION

I hereby declare that the work being presented in this thesis report entitled “**Solution processed Zinc Indium Tin Oxide Thin Films for Thin Film Transistor Applications**” by me in partial fulfilment of the requirements of the award of degree of **Master of Science in Physics** from **School of Physics and Materials Science**, Thapar University, Patiala is an authentic record of my work carried out under the supervision of **Dr. B.C. Mohanty, Associate Professor, School of Physics and Materials Science, Thapar University**.

ACKNOWLEDGEMENTS

I would like to express my deep sense of gratitude to Dr. B.C. Mohanty, *Associate Professor School of Physics and Materials Science, Thapar University, Patiala* for his invaluable suggestion, excellent supervision, constant encouragement, thought provoking and unabashed discussion in nurturing the work and during the preparation of manuscript throughout the research work.

My sincere thanks to Dr. Manoj Kumar Sharma, *Professor and Head, School of Physics and Materials Science, Thapar University, Patiala* for providing me with the opportunity to conduct this work and bring it out in the present form.

I offer special thanks and regards to Ms. Indu Gupta and Mr. Jasjit Singh, *Research Scholars, School of Physics and Materials Science, Thapar University, Patiala* for providing immense support in performing, characterizing and evaluating the thesis work.

I would also like to thank my friends (Preeti Gupta and Anisha) for their kind support and encouragement.

The greatest thanks go to my family members for their infinite support at each and every part of my life. Above all, I express my indebtedness to the almighty for all his blessing and kindness.

Nidhi
301404015

ABSTRACT

Zinc indium tin oxide thin films were grown on glass substrates by spin coating process. Zinc acetate dihydrate, indium chloride, and tin chloride dihydrate were used in aqueous solutions as the ion sources of In, Zn and Sn. $\text{In}_{2-2x}\text{Zn}_x\text{Sn}_x\text{O}_{3\pm\delta}$ films were grown for different value of x vaies from 0.1 to 0.4 with annealing temperature of 250-400 °C. The properties of the resulting thin films were characterized by various techniques such as X-ray diffraction (XRD), Field-emission scanning electron microscopy (FE-SEM) and optical absorption measurements. The film surface is covered with very fine nano-sized particles. The zinc indium tin oxide films grown were amorphous in nature and had a band gap of 3.25 eV. The films exhibited very high transmission better than 90% in the visible portion of the electromagnetic spectrum.

CONTENTS

Page no.

Chapter 1: INTRODUCTION	1
1.1 Thin film transistor (TFT)	1
1.2 Structure of TFT	2
1.3 Transparent electronics	3
1.4 TFT based on transparent conducting oxides (TCOs)	3
1.5 TCOs as channel layer	4
1.6 Potential candidates for channel layer	4
1.6.1 Zinc oxide(ZnO)	4
1.6.2 Tin oxide (SnO ₂)	5
1.6.3 Indium tin oxide (ITO)	5
1.6.4 Zinc tin oxide (ZTO)	6
1.6.5 Zinc indium oxide (ZIO)	7
1.6.6 Indium gallium zinc oxide (IGZO)	7
1.7 Amorphous zinc indium tin oxide as channel layer	7
1.7.1 Structural properties of zinc indium tin oxide	8
1.7.2 Optical properties of zinc indium tin oxide	9
1.8 Literature review of zinc indium tin oxide	9
1.9 Motivation and objectives	11
1.10 Solution based deposition technique for growing zinc indium tin oxide thin films	11
Chapter 2: EXPERIMENTAL TECHNIQUES	14
2.1 Growth of zinc indium tin oxide thin films	14
2.2 Characterization techniques	16
2.2.1 Structural characterization using X-Ray diffraction (XRD)	16
2.2.2 Surface microstructure studies	16
2.2.2.1 FE-SEM	17
2.2.3 Optical transmittance and band gap measurements	17

Chapter 3: CHARACTERIZATION OF ZINC INDIUM TIN OXIDE THIN FILMS	20
3.1 Evaluation of crystal structure	20
3.2 Evaluation of surface microstructure	21
3.3 Optical properties of zinc indium tin oxide thin films	22
Chapter 4: SUMMARY AND FUTURE SCOPE	25
REFERENCES	26

LIST OF FIGURES

Figure	Title	Page number
1.0	Schematic cross-sectional view of a modern TFT	2
1.1	Typical phase diagram of the zinc indium tin oxide compound	9
1.2	A schematic of the spin-coating process	13
2.1	Snapshots of the cation precursor solutions.	14
2.2	Snapshot of the precursor solution ready to be deposited on the substrates.	15
2.3	Photograph of the spin-coater used in this work.	15
2.4	Illustration of the constructive interference of the X-rays scattered from lattice planes.	16
2.5	Single Beam UV-visible spectrophotometer	19
2.6	Double Beam UV- visible Spectrophotometer.	19
3.1	Typical XRD patterns of the zinc indium tin oxide thin film	20
3.2	FE-SEM images show very smooth surfaces of the zinc indium tin oxide thin films.	21
3.3	FE-SEM images at higher magnification showing surfaces of the zinc indium tin oxide ($x = 0.3$) thin films. The cross-sectional image is also given, which shows the thickness to be ~ 95 nm.	22
3.4	Transmittance (%) spectrum of the zinc indium tin oxide thin film with $x = 0.1$ to 0.4	23
3.5	Plot of $(\alpha h\nu)^{1/2}$ vs $h\nu$ for the zinc indium tin oxide thin films with $x = 0.1$ and 0.3 .	24

CHAPTER 1

INTRODUCTION

Over the years, thin films technology has evolved into a major research theme world-wide owing to the use of thin films in a wide area of applications such as microelectronic devices, optical coatings, data storage media, flat panel displays, photovoltaic cells, sensors, etc. A thin film is a two dimensional layer material deposited typically by the process of condensation and growth of atoms, molecules or ions on substrate materials such metals, ceramics or polymers. There are many deposition techniques for depositing the thin film on the substrate material and each one has its advantages and disadvantages [1].

In the last few decades, research on thin film transistors (TFTs) has gained tremendous attention owing to the growing popularity of electronic devices and the miniaturisation of the devices. Correspondingly, thin films of a number of materials grown using different deposition techniques have been evaluated for possible layers in the TFT. Recently, there has been growing interest in preparing transparent TFTs, for which many materials in the form of thin films have been extensively studied.

1.1 Thin Film Transistors (TFT)

TFT is a special kind of field effect transistor (FET). The structure and operation is very similar to the metal oxide field effect transistor (MOSFET), which is one of the important device components in integrated circuits (ICs) and its potential utility can be traced back to the 1930s when the invention of the TFT was patented. In 1962, RCA laboratories reported the fabrication of a TFT using thin films of polycrystalline cadmium sulfide (CdS) as the semiconductor material. Silicon-based TFTs have become the important devices for active-matrix liquid crystal displays (AMLCDs) in 1980s. In the past ten years, amorphous silicon (a-Si:H) TFTs have successfully dominated the large-area LCD product market. The first functional TFT made from hydrogenated amorphous silicon (a-Si:H) in 1979 with a silicon nitride gate dielectric layer. The films were deposited by plasma-enhanced chemical vapor deposition (PECVD) technique, this technique easily carried out in large-area and low-temperature glass substrates. There were some drawbacks in the a-Si:H TFT device. Firstly for large-current applications the mobility was too low of this TFTs. Secondly under light exposure conditions these TFTs had large leakage

current and thirdly this TFT are not very effective for large-area production process for the high mobility with good reliability. Over 14 or 15 years there is huge advancement in the field of TFT technology. Now these days' industries are focused on the lowering production cost, and large area production. Recently the researchers being studied about new generation of oxide semiconductors and applied it as the active material to the TFT device, particularly the zinc oxide (ZnO) based TCOs and indium gallium zinc oxide (IGZO) thin films. [2]

1.2 Structure of TFT

TFT is the three terminal (gate, source and drain) field-effect transistor device. The working of TFT depends on the flow of current through the semiconductor which is in-between the source and drain electrode. An insulator is placed in mid of gate electrode the semiconductor. The most common TFT structure is given in **Figure 1.0**.

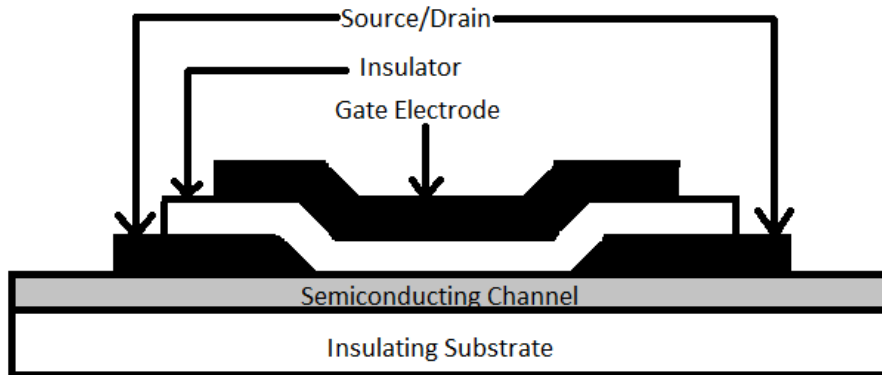


Figure 1.0: Schematic cross-sectional view of a modern TFT

TFTs are similar to MOSFETs in terms of their basic principle. However, important differences exist between TFTs and MOSFETs device. TFTs are formed on the insulating material which includes glass substrate and the silicon wafer in MOSFETs used as the substrate as well as the semiconductor. The great performance should be seen in MOSFETs because of the flow of electrons take place in single crystalline and leads to high mobility whereas; in TFTs the material using is polycrystalline or amorphous in nature. Also, the fabrication temperature of both devices is quite different. In deposition of MOSFETs temperatures exceeding 1000 °C whereas in TFTs the temperature should not to be exceed from certain ranges of the substrate.

For example, the common glass substrate has temperature range from 600-650 °C. In MOSFETs p-n junctions is formed around source and drain regions, while in TFTs there is not such p-n junctions. The TFTs have two types of structures which are staggered and coplanar. These two types are further divided into top-gate and bottom-gate structures, depending on the level of gate electrode of the structure. In top-gate structure the gate electrode is on top of the semiconductor layer and in bottom-gate structure the gate electrode is below the semiconductor layer. These structures had its advantages and disadvantages. For example, in the a-Si:H TFTs staggered bottom-gate structure is commonly use, because it can easily prepared and fabricate and have great electrical properties. On the contrary, a coplanar top-gate configuration is usually preferred for polycrystalline Silicon TFTs. The bottom gate structure is more attractive than the top gate structure because the fabrication is continuous in bottom gate structure while it is not possible in top gate structure since Semiconductor Island be patterned before the gate oxide is form. Bottom gate structure can easily be cleaned while top gate structure needs extra care for cleaning [3-4].

1.3 Transparent electronics

Transparent electronics is become a famous and advanced topics in science and technology field which is focused on producing wide range of opto-electronic device applications. The semiconductors having wide band-gap in which the oxides of different chemical components is the key component of the transparent electronics and play a valuable role, as passive component as well as the active component. It is one of the most promising technologies for future electronic devices. To achieve the transparent electronic devices we have to discover and to understand the material that it should be optically transparent and electrically conductive. Then implement and evaluate in transistor or other invisible circuitry devices. Last one is to achieving its applications and other properties. To understand transparent electronics it requires all the other technology to bring together. The classes of materials that have been available for transparent electronics applications have grown dramatically. Transparent electronics now is dominated by the transparent conducting oxides [4-5].

1.4 TFT based on transparent conducting oxides (TCOs)

TCOs have been used for several years and it is very important material for photovoltaic devices and optoelectronic applications. TCO thin films of indium tin oxide, zinc oxide, tin oxide

and these mixtures have highly desirable. The fabrication of amorphous TCOs (ATCOs) is in interest as the deposition of amorphous material takes place at lower temperatures than crystalline and the manufacturing on different range of substrate such as plastic. This new class of semiconductor materials, amorphous oxides semiconductors (AOS) represents a revolutionary idea which exhibits a combination of high optical transparency and high electron mobility. There is an advantage for process synthesis of AOSs because do not have grain boundaries due to which they have surface smoothness and compositional uniformity. Other than these advantages the materials which are using is environmental friendly and less expensive. During the last thirty, tin oxide (SnO_2), indium oxide (In_2O_3), indium tin oxide (ITO), and zinc oxide (ZnO) are being dominant TCOs in thin film industry. Electron beam evaporation, chemical vapor deposition, pulsed laser deposition; spray pyrolysis, sputtering and sol-gel methods are the variety of deposition techniques by which TCO thin films can be prepared [6-7].

1.5 TCOs as channel layer

Amorphous oxide semiconductors, is the favourable materials for the channel layer in TFT. The typical channel layer materials having amorphous oxides composed of heavy-metal cations with $(n-1)d^{10}ns^0$ electronic configurations. The ns^0 orbital has spherical symmetry; these orbitals diffuse together and give higher mobility. The filled d-d electronic transition gives visible region in electromagnetic spectrum. The most famous cations which are used in channel layer are Zn^{2+} , Cd^{2+} , In^{3+} , and Sn^{4+} and to some lesser amount Ga^{3+} due to gallium oxides have large band-gap and lower. In TFTs TCOs are used as channel layers because of its high-performance devices which is due to high electron mobility and excellent electrical characteristic [8].

1.6 Potential candidates for channel layer

1.6.1 Zinc oxide (ZnO)

ZnO is a wide-band gap semiconductor having band gap ~ 3.37 eV with hexagonal wurtzite structure. ZnO has several favourable properties, including good transparency and high electron mobility. ZnO is attractive for thin film material due its good polycrystalline nature and it can fabricate at room temperature on plastic or flexible substrate and the ZnO is also less light sensitive material [9].

In 2003, Hoffman et al. fabricated ZnO-based highly transparent thin-film transistors of optical transmission of 75% in visible electromagnetic spectrum. By ion beam sputtering the ZnO channel layer and ITO source/drain electrode were deposited on the substrate. The substrate was not heated during deposition. After that the ZnO layer undergoes rapid thermal anneal at 600 - 800 °C in O₂ in order to enhance the resistivity of channel, electrical properties, and increase the crystalline nature of the ZnO channel. To increase in transparency of the thin film ITO/ATO is deposited under rapid thermal annealing at 300 °C in O₂ [10].

Furthermost, in 2003 Carcia et al. demonstrated ZnO thin film transistor fabricated on Si substrates at room temperature using ZnO as a target by RF magnetron sputtering technique. The prepared films had resistivity of $\sim 10^5$ ohm cm and optical transmission greater than 80% in visible region of em spectrum. The transparency in the visible region of electromagnetic spectrum and processing low-temperature makes ZnO thin-film transistors effective for the flexible electronics where the substrates are temperature sensitive [11].

Norris et al. fabricated TTFT using ZnO as the channel layer synthesised by spin-coating deposition. The zinc nitrate based precursor solution is spin onto substrate of indium tin oxide/aluminium tin oxide, and then thin layer of ZnO was baked in air at 600 °C for 10 minutes. A rapid thermal annealed is done in presence of oxygen at 700 °C to improve the film crystallinity. Spin-coated ZnO TTFTs manufactured is lighter sensitive than devices fabricated by ion-beam sputtering which means there is higher degree of surface roughness in the channel layer formed by the spin-coated technique [12].

1.6.2 Tin oxide (SnO₂)

The SnO₂ TFTs fabricated by Klasens and Koelmans, Aoki and Sasakura, Prins et al. and Wollenstein et al. were the depletion mode devices which required the gate voltage to turn them off. In 2004, Presley et al. fabricated SnO₂ as channel layer in TTFT which was deposited via magnetron sputtering technique by using tin oxide as a target, and then rapid thermal annealed at 600 °C in O₂. The enhancement-mode bottom-gate structure TTFT was developed. The channel layer is approximately 10 - 20 nm. The thin film having transparency of $\geq 90\%$ across the visible spectrum but with the substrate the transmission is 75% across visible spectrum [13].

1.6.3 Indium tin oxide (ITO)

ITO is widely used in optoelectronic devices. Tin doped indium oxide (ITO) films are one of the most used TCO because these thin films are highly transparent in the visible spectra and have superior conductivity. This is why they are used as electrode material in flat panel display. The ITO films properties are strongly depend on the deposition techniques. There is a wide variation in band gap values as well as the dopant concentration among other properties and parameters have been the reported. Few researchers explored that ITO can be deposited on low temperature substrates by various deposition techniques included RF magnetron sputtering, physical vapor deposition, chemical vapor deposition and sol-gel deposition [14].

Jeon et al. in 2010 fabricated ITO films by sol gel method in which the precursor is annealed at 500 °C in air for 2h after spin coating. Aluminium is added to the ITO for effective use of indium oxide as TCO. The thin films of indium tin oxide which was prepared by the sol-gel method were transformed to a semiconductor by addition of Al into the composition to increase the band gap and due to which the band gap changes from 3.3 to 4.0 eV [15].

1.6.4 Zinc tin oxide (ZTO)

Chiang et al. in 2005 prepared a TFT using ZTO, as the channel layer because of its amorphous nature and wide band gap. The ZTO and ITO was deposited using radio frequency magnetron sputtering at substrate temperature of 175 °C. It has been seen that ZTO found to be amorphous up to 650 °C post deposition annealing temperature above it ZTO shows crystalline nature. The optical transmission shows the transmission of ~84% in visible spectrum [16].

A methodology for the passivation of TFT utilizing zinc tin oxide as the channel layer and silicon dioxide as the passivation layer is developed by Hong et al. This method involves annealing of the TFT when channel layer deposition takes place and then additional annealing take place after thermal evaporation of a SiO₂ passivation layer at 600 °C. Hong et al. demonstrated ZTO TFTs were fabricated by using a metallic zinc/tin alloy as a sputter target via magnetron sputtering [17]. At last, Hoffman researched the effects variation of sputter target stoichiometry and annealing temperature on which film is deposit on the properties of zinc tin oxide [18].

In 2009 ZTO thin films were fabricated through spin-coating which was simple and had low-cost precursor solution. The films were annealed at 400 and 500 °C. By this method film was continuous and uniform. They exhibit $\geq 90\%$ transparency and were amorphous in nature.

For good transistor characteristics and flexible field-effect transistors zinc tin oxide thin films as channel layer in TFTs have been used. [19].

1.6.5 Zinc indium oxide (ZIO)

Due to its excellent optical transmission, chemical stability, thermal stability, high electrical conductivity and surface smoothness amorphous ZIO become a valuable TCO. In 2005, Dehuff et al. fabricated n-type TFTs using ZIO as a channel which was deposited via radio frequency magnetron sputtering. The optical transmissions of TFT were > 85% in the visible spectra of the em spectrum and have high mobility. The XRD analysis shows that the channel layers of zinc indium oxide TTFT at 500 °C remains amorphous and for 600 °C its turns to be polycrystalline. High performance TTFT channel is low temperature processed ZIO amorphous oxides [20].

In 2006, Barquinha et al. fabricated TTFTs with the channel layer of ZIO by RF magnetron sputtering at room temperature in which film thicknesses of 15 - 60 nm were produced. Optical transmission reveals that transparency > 80%, including glass substrate across the visible region of the electromagnetic spectrum [21].

1.6.6 Indium gallium zinc oxide (IGZO)

For channel layer material of TFTs indium gallium zinc oxide (IGZO) is a good alternate. Due to the large band gap and having higher mobility, IGZO is transparent in the visible region. IGZO is amorphous in nature but have high mobility is due to presence of s-electrons conduction [22].

Nomura et al. in 2003 demonstrated a transparent TFT using channel layer of a single crystalline a-IGZO. The pulsed laser deposition technique (PLD) is used to fabricate onto a single crystal of YSZ substrates. The TTFTs were fabricated at 700 °C temperature. The optical transmittance of these thin films is >80% including substrate [23]. So far; most of the IGZO TFTs which are fabricated is deposited only by magnetron sputtering and pulsed laser deposition in order to reduce the cost the films they are fabricated by spin-coating.

1.7 Amorphous zinc indium tin oxide as channel layer

Zinc indium tin oxide is the promising replacement for indium tin oxide as the transparent conducting oxide layer in many opto-electronic applications. Zinc indium tin oxide contains less amount of indium than ITO as the codoping of zinc and tin take place, which lowers the production cost, and gives us the better option for compositions that let the TCO layer to be adjusted for each application. Phillips et al. was the first who reported the fabrication of zinc indium tin oxide in 1995, of polycrystalline oxide as a target by PLD technique. Numerous films in the ZnO-In₂O₃-SnO₂ (ZITO) have been grown and their electrical and optical properties are being studied by varying the composition and changing in the deposition methods [24].

In the followings a brief literature review on Zinc indium tin oxide is presented.

Properties of zinc indium tin oxide

1.7.1 Structural Properties of zinc indium tin oxide

The subsolidus phase relationships in the ZnO–InO_{1.5}–SnO₂ system were investigated at 1275 °C using X-ray diffraction. **Figure 1.1** shows the reported phase diagram of the compound. In the ternary diagram end members consist of transparent conducting oxides which are zinc oxide, indium chloride and tin oxide. This subsolidus phase relation of ZITO do not show any ternary compound, but two solid solutions is of particular interest. The bixbyite solid solution In_{2-2x}Zn_xSn_xO₃ (x = 0-0.40), and the indium substituted zinc stannate spinel, Zn_(2-x)Sn_(1-x)In_{2x}O₄ (x = 0-0.45) are the two substantial ternary phase space solution. The bixbyite ZITO is an excellent conducting TCO, whereas the spinel ZITO has poor conductivity and it keeps on decreasing as In content goes on increasing. Along with these two there is ZnO–InO_{1.5} binary TCO homologous compounds series (ZnO)_k.In₂O₃ (where k = 3, 4, 5, 6, 7, 9, 11). ZnO–InO_{1.5} binary does not observe any compound up to temperature of 1325°C. It has been seen that if we replaced 40% of the indium with Zn and Sn in bixbyite phase (x = 0.4 in In_(2-2x)Sn_xZn_xO₃), it still maintains its bixbyite nature. And still remain an outstanding TCO. In bixbyite solid solution specimens there is decrease across the solution range i.e. the In component In₂O₃ to x = 0.4 In_{2-2x}Zn_xSn_xO₃, and also there is decrease in the lattice parameter. For ZITO thin films have been fabricated from different compositions by a variety of deposition techniques. Some of the thin films are fabricated with non equilibrium components their characteristics will be same as that of the bulk material [25].

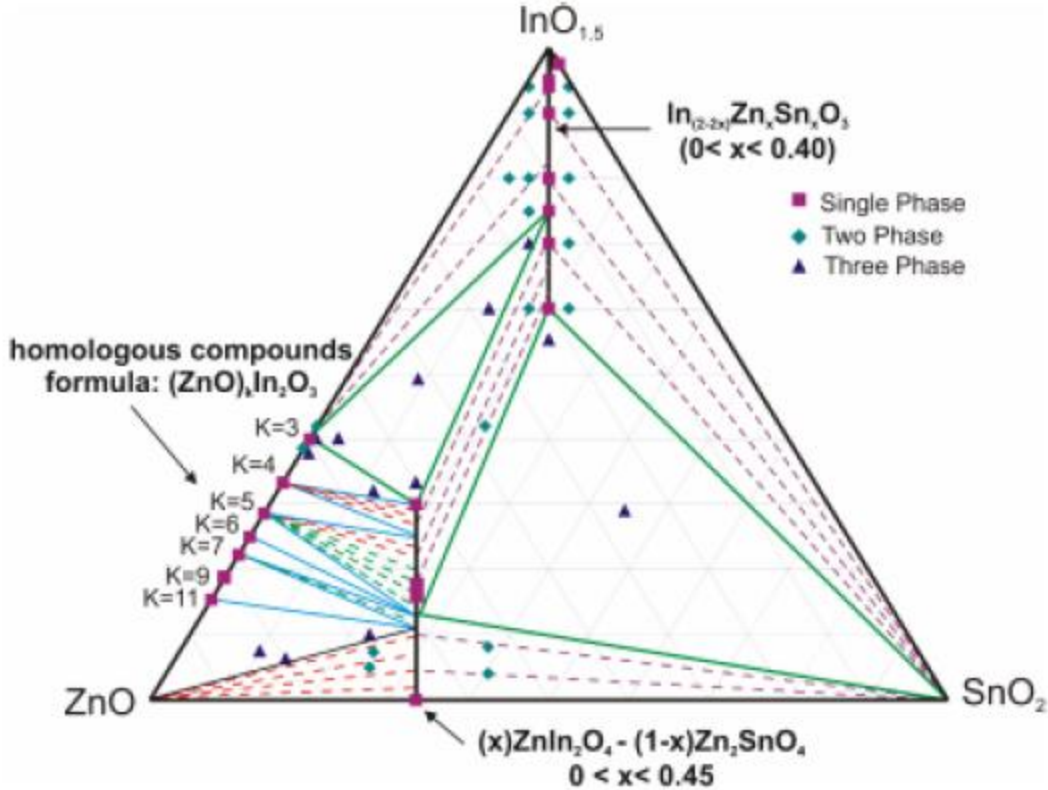


Figure 1.1: Typical phase diagram of the zinc indium tin oxide compound [24]

1.7.2 Optical Properties of zinc indium tin oxide

Although the zinc indium tin oxide films deposited in different temperatures but it appears to be almost seen to be identical. Particularly the optical absorption can identify by Tauc plot, which reveals difference between the amorphous and crystalline nature of thin films. To determine the energy band gap a plot of between $(\alpha h\nu)^{1/2}$ vs $h\nu$ is plotted. Zinc indium tin oxide is considered to be a direct band-gap semiconductor. An analysis by Tauc et al. it concluded Bloch functions is the linear combination of the crystalline wave-functions of the respective bands, and hence momentum, $\hbar k$, is not conserved for amorphous material even in a direct transition. For highly crystalline ZITO at $x=0.3$ the band-gap reported is $\sim 3.8\text{eV}$. [26]

1.8 Literature Review on zinc indium tin oxide (ZITO)

In 2007 Ow-Yang et al. demonstrated amorphous ZITO films by direct current magnetron sputtering onto glass substrates. The constituents of the ceramic oxides Zn:In:Sn cation having different ratios. The analysis of XRD showed that the ZITO remains amorphous during annealing at $200\text{ }^\circ\text{C}$. Optical transmission have transparency of films is $> 80\%$ is shown

in electromagnetic spectrum in the visible region. The energy band-gap was in range of 3.52–3.74 eV. These thin films used organic light emitting diodes (OLEDs) applications. The thin film prepared is more effective than the tin and zinc doped In_2O_3 [27].

In 2007, Zhang et al. developed $\text{Zn}_{0.3}\text{In}_{1.4}\text{Sn}_{0.3}\text{O}_3$ (ZITO) thin films by pulsed laser deposition (PLD) on Aluminium oxide substrates. Transmission electron microscopy (TEM) shows that the ZITO films were composed of twin-related domains with their planes parallel to planes of the Al_2O_3 substrate in its cross-section and plan-view [28].

Grover et al in 2007 prepared TFTs with transparent amorphous zinc indium tin oxide as a channel layer. The optical transmittance of the channel layer is ~85% in the visible region. The channel layer is fabricated by RF magnetron sputter technique and then the thin film is annealed in furnace in presence of air. The XRD patterns for ZITO films indicate up to annealing temperature of 600 °C the film is amorphous in nature. The crystalline nature of thin film is observed at the deposition annealing temperature of 650 °C [29].

In 2009, Ryu et al. researched the effect of the Sn/Zn ratio on the gate voltage stress-induced stability in the amorphous ZITO system. The stability of the TFTs dramatically improved with a change composition of channel to Zn:In:Sn = 0.35:0.20:0.45 while other devices with composition Zn:In:Sn = 0.45:0.20:0.35 and 0.40:0.20:0.40 experience deep level trap creation and charge trapping in the channel, respectively. Therefore, in the amorphous ZITO network, Sn atoms act as stabilizing agent [30].

Buchholz et al. in 2009 fabricated ZITO films by PLD in which 30% of the In in the indium oxide structure is substitution with Zn and Sn in equal molar proportions: $\text{In}_{2-2x}\text{Zn}_x\text{Sn}_x\text{O}_3$, when $x = 0.3$. Analysis shows that XRD patterns of the films grown have amorphous nature up to 100 °C. At 200 °C of deposition temperature, crystalline nature of thin films begins to appear and becomes clearly seen in deposition temperature of 400 °C. The change in the crystalline nature of the ZITO film affects the electrical properties, and also the grain boundaries [8].

In 2011, Carreras et al. prepared samples by sputtering of ZnO and ITO targets. The samples were deposited by RF sputtering technique in which varying RF powers is given to the ZnO which is target while ITO target kept constant. The zinc content ratio is varying from 0 to 67%. The thin films prepared with 17% Zn content ratio shows the lowest resistivity and the highest transmittance > 80% in the visible region of electromagnetic spectrum. X-ray Diffraction studies show the prepared thin film is amorphous material. As on increasing the Zn content in

sample the amorphous nature tends to increase. The samples have the sample electrical properties after one year when kept in normal atmosphere [31].

Also in 2012, Buchholz et al. fabricated ZITO films by PLD with three different material in which ZITO is consists of 30%, 50% and 70%, respectively, of the In which is substitute with Zn and Sn in equal molar concentration $\text{In}_{2-2x}\text{Zn}_x\text{Sn}_x\text{O}_3$, where $x = 0.3, 0.5, 0.7$. The grown ZITO thin films were amorphous in nature at room temperature. The crystalline nature of ZITO film is seen at higher deposition temperature and increased as there was increase in the co-substituent of Zn and Sn in indium oxide [32].

Marsal et al. in 2014 developed ZITO layers with different compositions for use as the active layer in TFTs. ZITO samples were deposited over the Si wafers by radio frequency magnetron co-sputtering of zinc oxide and indium tin oxide as sputter target at room temperature. One sample of each kind was annealed in air atmosphere. Each sample was heated during 1 h at 300 °C, with a temperature ramp-up of 30 min. The aim of the thermal treatment was to oxidize the film to decrease the carrier concentration by reducing the oxygen vacancy density of oxygen at the ZITOs surface and nano-grain boundaries. The X-Ray diffraction analyzed and high-resolution transmission electron microscopy results showed that the structure is not completely amorphous, but have some nanocrystals particles [33].

1.9 Motivation and objective

The brief literature survey presented above shows that ZITO has evolved as a promising material for transparent TFTs owing to its suitable and tuneable electrical, optical and structural properties. However, one can find that preparation of these thin films involves high cost vacuum techniques including PLD and sputtering. The solution based techniques, which are traditionally considered as scalable techniques for deposition on large area substrates, have been somewhat less explored in the growth of the ZITO thin films, and forms the basis of this work. The objectives of this work are as following:

- Growth of ZITO thin films using a simple solution techniques such as spin-coating
- Investigation of structural, surface morphology and optical properties of the resulting films to check their suitability in the TFT applications.

1.10 Solution based deposition techniques for growing zinc indium tin oxide thin films

The sol-gel process is a versatile process for the growth of various thin films using chemical solutions. The sol-gel process involves of a system undergoes transition from a liquid into a solid phase. The sol-gel method has many advantages for the synthesis of a large variety of thin films and coatings and involves chemical and physical processes. It consists first in preparing a solution of inorganic or organometallic precursors or metal oxide particles dispersed in a solvent. The sol can be spread across the substrate by different techniques. The two most widely used techniques: dip coating and spin coating [34].

Spin coating is widely used in semiconductor industry, creating thin films of few nm of even quality. The physics of spin coating can be effectively modelled by dividing the whole process into three stages, which are deposition, spin-up and evaporation of solvents. Stage 2 and stage 3 are the two stages that have important on final coating thickness. A schematic of the deposition process is given in **Figure 1.2**.

Stage 1 Deposition:

In deposition stage, the solution is deposit at centre of the substrates micro syringe or dropper drop-wise. The number of drops depends on the viscosity of the solution and size of the substrate be coated. Then depending on the viscosity of solution the substrate is accelerated to its desire speed. The solution is spread out due to centrifugal force and height is reduced to that of critical height.

Stage 2 Spin-up:

The second stage is spin up in this stage the substrate is accelerated in the desired acceleration. In this stage excess of solution is expelled from the substrate. The rotation of the substrate at high speed means that centripetal force combined with the surface tension of solution pulls the liquid coating into even covering.

Stage 3 Evaporation:

The third and final stage is evaporation or drying. The film starts drying from the time when centrifugal out flow stops and there is shrinkage of the solvent on the substrate because of the solvent loss. This results in the formation of thin film on the surface of the substrate. For

thick films it takes long drying time which increases the physical stability of the film before handling [35].

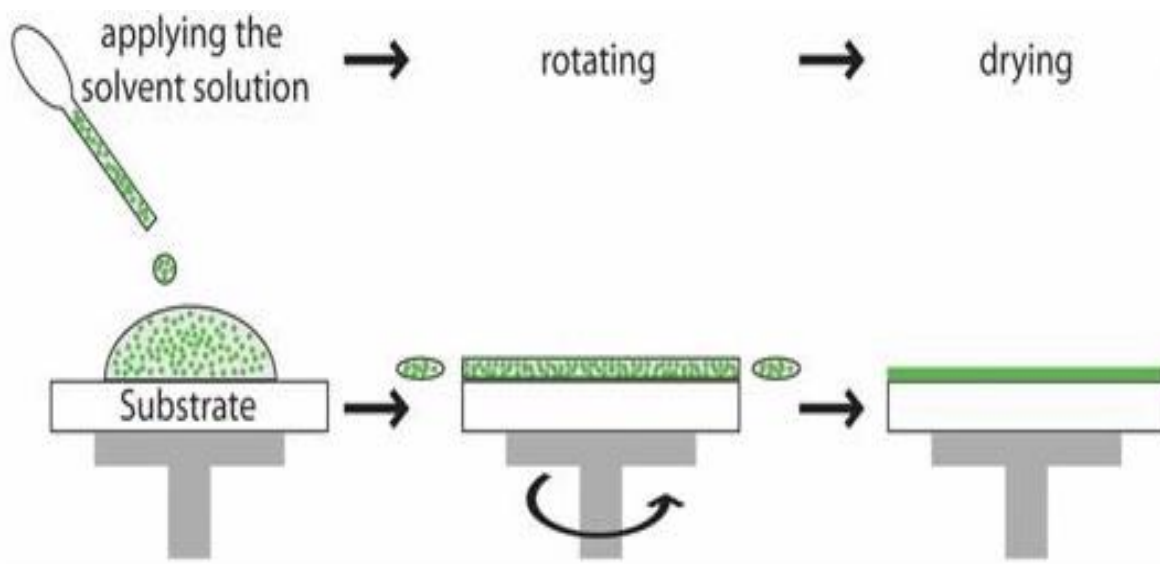


Figure 1.2: A schematic of the spin-coating process [36]

CHAPTER 2

EXPERIMENTAL TECHNIQUES

In this chapter, experimental technique used to grow and characterize the ZITO thin films have been presented. Section 2.1 gives a brief description about the film preparation. Section 2.2 gives the detail of various techniques which are used for characterisation of thin films.

2.1 Growth of zinc indium tin oxide thin films

Thin-films of ZITO specimens were grown by the spin coating deposition technique on the glass substrates. The intended target composition was $\text{In}_{2-2x}\text{Zn}_x\text{Sn}_x\text{O}_{3\pm\delta}$, with $x = 0.1-0.4$. Zinc acetate dihydrate (98%), indium chloride (98%), and tin chloride dihydrate (99.9%) in various $\text{Zn}^{2+}:\text{In}^{3+}:\text{Sn}^{4+}$ molar ratios are dissolved in 10 mL of 2-methoxyethanol (99%) separately. **Figure 2.1** shows snapshots of the cation precursor solutions.



Figure 2.1: Snapshots of the cation precursor solutions.

The overall metal cation concentration remained 0.3 M. Then, the solutions were mixed well by using magnetic stirrer. The sequence of the adding solutions is zinc acetate dihydrate, indium chloride and then tin chloride dihydrate under continuous stirring of 450-500 rpm for total metal concentration. Then, add ethanolamine (99%) which acts as the stabilizing agent in 5 mL of the prepared mixed solutions, maintaining the ethanolamine:total metal concentration in a 1:1 molar ratio. This clear solution obtained is then stirred for 2 h on the magnetic stirring bar at room temperature at 500 rpm before the solution put it for spin-coating. The glass slide which is

used as substrate is first wash with detergent solution, then ultrasonic cleaning in DI and lastly cleans with acetone for 10 min. **Figure 2.2** shows snap shots of the precursor solution ready to be deposited on the substrates.

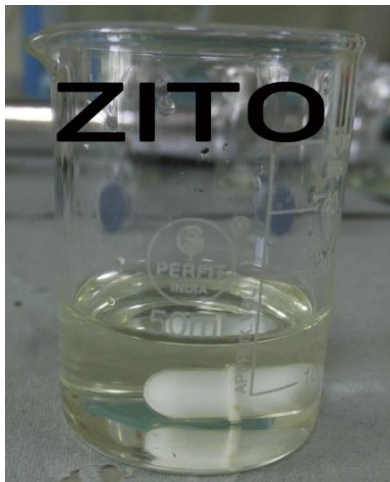


Figure 2.2: Snapshot of the precursor solution ready to be deposited on the substrates.

The prepared metal precursor solution with different metal compositions is then spin-coated on the substrates at a speed 4000 rpm with acceleration of 10 rpm/s in time of 30 seconds. The coated films were then annealed on a hot plate at 250-400 °C under air for 10 min. To increase the film thickness the deposition process is repeated for two or three times [37]. The spin-coater used in this work is shown in **Figure 2.3**.



Figure 2.3: Photograph of the spin-coater used in this work.

2.2 Characterization techniques

2.2.1 Structural characterization using X-Ray diffraction (XRD)

XRD is a rapid analytical technique which primarily used to identify the phase of crystal structure of materials and information about the unit cell dimensions. It is a common technique in studying the atomic spacing in the crystal. XRD analysis is based on constructive interference of monochromatic X-ray and crystal structure of the material. When X-ray are scattered from the crystal lattice it produce constructive interference only if it satisfies the Bragg's condition which is:

$$n\lambda = 2d \sin\theta$$

Here n is an integer and d is inter planar spacing between the crystal

This law gives the relation between the wavelength and lattice spacing in the crystal. XRD analysis can identify fine-grained minerals as clays which are difficult to indentify optically and determination of unit cell dimensions measurement of sample purity. The different phases of the crystal also can be analysed by the X-ray analysis. The average intermolecular spacing between layers of crystal can be identifying. The other parameters of the crystal lattice can be identified from the XRD data analysis software. **Figure 2.4** shows a schematic diagram illustrating the basic principle of XRD.

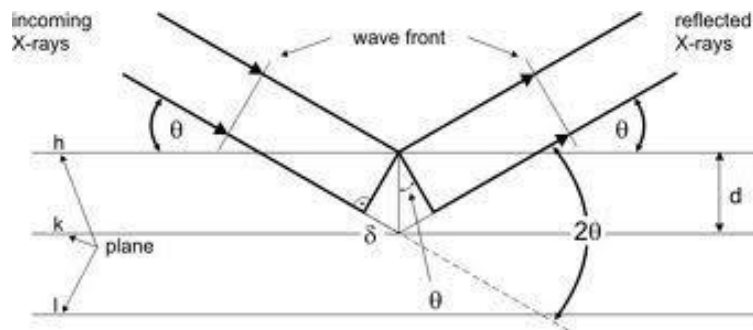


Figure 2.4: Illustration of the constructive interference of the X-rays scattered from lattice planes.

2.2.2 Surface microstructure studies

Topographical and elemental information at higher magnifications with virtually unlimited depth of the thin films were studied under field emission scanning electron microscopy (FE-SEM). FE-SEM is high resolution electron microscopy.

2.2.2.1. FE-SEM

A FE-SEM is microscope which uses a beam of electrons instead of light to generate the image or analysing the specimen. The FE-SEM uses raster technique in order to get image of the sample. With the help of the high energy electron beam there is interaction between electrons and the atoms in the sample and gives information in form of signal about surface topography and composition. It can observe small area contamination spot of few nanometres. The thickness measurement of thin films, surface morphology, measurement of height and dimensions of sample and analysis of fracture are the some applications of FE-SEM. The working of FE-SEM is depends on electron emitters emission gun which can produce emission from tungsten filament up to 1000x. But in FE-SEM vacuum conditions should be higher. When electrons beam strike on the sample the beam is a confined monochromatic beam which is focused on a very small area using metal apertures and magnetic lenses. Finally, detectors will collect the electrons and signals are produce an image of the specimen [38-42].

2.2.3 Optical transmittance and band gap measurement

To study the optical absorption particularly the optical gap and absorption discontinuity in absorption spectrum of the specimen UV-visible-NIR spectroscopy is used. To analyze the interactions between radiation and matter in the UV-visible region of the electromagnetic spectrum ultraviolet (UV)-visible spectrometers are used. The principle of UV-visible-spectroscopy is that UV absorption spectrum which is due from transition of electron with in a molecule from lower level to an upper level, absorbs UV radiation of frequency ν . The instrumental equation for Beer-Lambert law is given as:

$$I = I_0 e^{-\alpha d} \quad \dots\dots (a)$$

Where, I_0 = intensity of the incident light

α = absorption coefficient

t = thickness of the thin film.

$$\alpha = -\frac{1}{t} \ln \frac{I}{I_0}$$

..... (b)

The transmittance (T) of the sample is given by ratio I/I_0 . So absorption coefficient is related to transmittance. The relation is given by:

$$\alpha = -\frac{1}{t} \ln T$$

..... (c)

The optical band-gap is related to absorption coefficient according to Tauc relation the following given equation of direct allowed transition,

$$\alpha = \frac{A}{h\nu (h\nu - E_g)}$$

Where $h\nu$ be the incident photon energy, A is a constant proportionality and E_g is the energy gap. The constant of proportionality is different for different transition. To determine the band-gap plot the graph between $(\alpha h\nu)^2$ and $h\nu$, the extrapolated linear portion intercept on x-axis gives the value of E_g .

With the help of the diffracting grating a light source which is visible light gets separated into its component wavelength. The half mirrored device split this componential wavelength into two beams. First beam i.e the sample beam, passes through a small transparent thin film on which deposition is done. The second beam is the reference, passes through a glass substrate on which no deposition is done. The detector can detect the intensity of these beams and compared them. In a short time, the spectrometer automatically scans all the component wavelengths.

Light source, a sample holder, a diffracting grating mono-chromator and a detector are components of spectrophotometer. The radiation source is often a Tungsten filament or more recently, light emitting diodes (LED) and the detector is simply a photomultiplier tube. With the help of single photodiode with scanning mono-chromators a light of monochromatic wavelength reaches at the detector one at a time. There are two types of spectrophotometer single beam and double beam. In a single beam, the light of intensity I pass through the sample cell, whereas I_0 measured by removing the sample. **Figure 2.5** shows the schematic arrangement of components in a single beam UV-visible spectrophotometer [43-46].

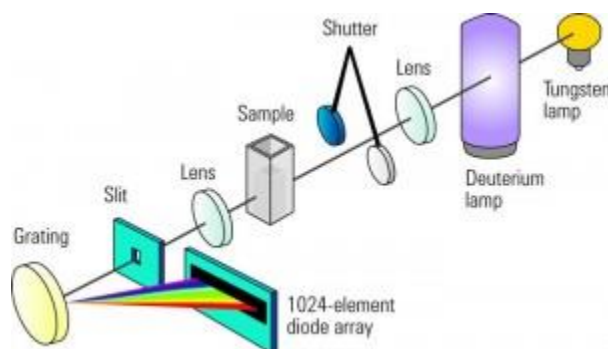


Figure 2.5: Single Beam UV-visible spectrophotometer

Double beam UV-visible spectrophotometer

The light constituting wavelength is divided into two beams in a double-beam spectrophotometer. The one beam is call reference beam which gives intensity of 100% of transmission I_0 and the other beam passes through the sample gives intensity I , and measurement is taken as the ratio of two beam intensities. **Figure 2.6** shows the schematic arrangement of components in a double beam UV-visible spectrophotometer [47].

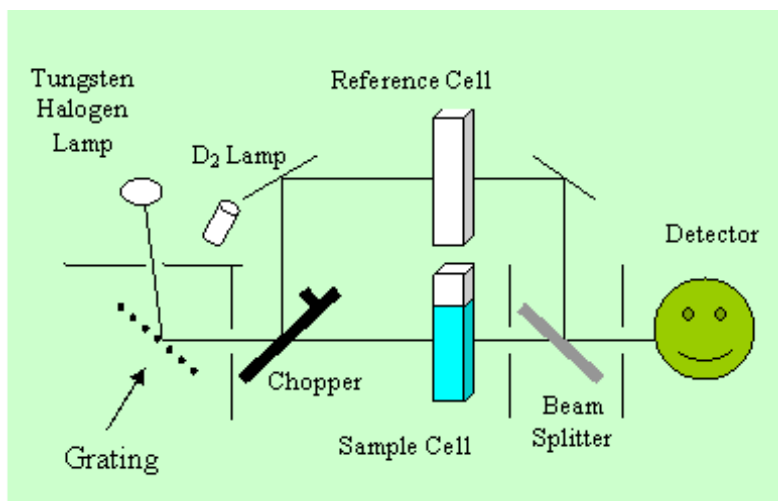


Figure 2.6: Double Beam UV- visible Spectrophotometer

CHAPTER 3

CHARACTERIZATION OF ZITO THIN FILMS

Evaluation of the properties of ZITO thin films

Following the experimental procedures outlined in chapter 2, ZITO thin films were prepared by the spin coating process and annealed at 250°C-450 °C. The results of the XRD, FE-SEM and UV-visible spectroscopy studies are presented in the following sections.

3.1 Evolution of crystal structure

A representative XRD pattern of the as-deposited ZITO thin films of different compositions with $x = 0.1$ to 0.4 grown by the spin coating process is presented in **Figure 3.1**. The figure shows featureless curves with no Bragg peaks for all compositions, which suggests that the as-deposited ZITO thin films grown by spin-coating are amorphous in nature.

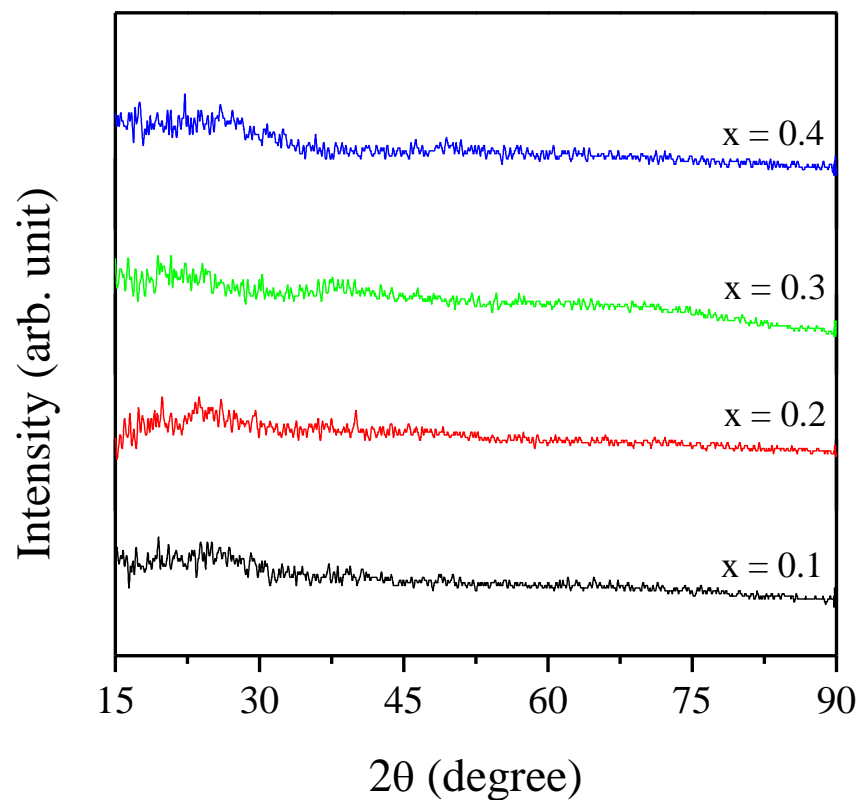


Figure 3.1: Typical XRD patterns of the ZITO thin film

3.2 Evaluation of surface microstructure

Surface characterization by FE-SEM revealed that all films irrespective of their composition are very smooth. For example, **Figure 3.2** shows the SEM micrographs depicting surface features of the ZITO thin films ($x = 0.2$ and 0.3). It is observed that the ZITO thin film covers the substrate well with occasional pin holes at random places. At high magnification, some particulate aggregation was observed on the surface of the films (white contrast in the micrographs). At higher magnification, it was revealed that the grains are of nano size leading to a locally smooth surface. **Figure 3.3** shows high magnification images of the films with $x = 0.3$. The thickness of the films was about 95 nm as revealed from the cross-sectional SEM images.

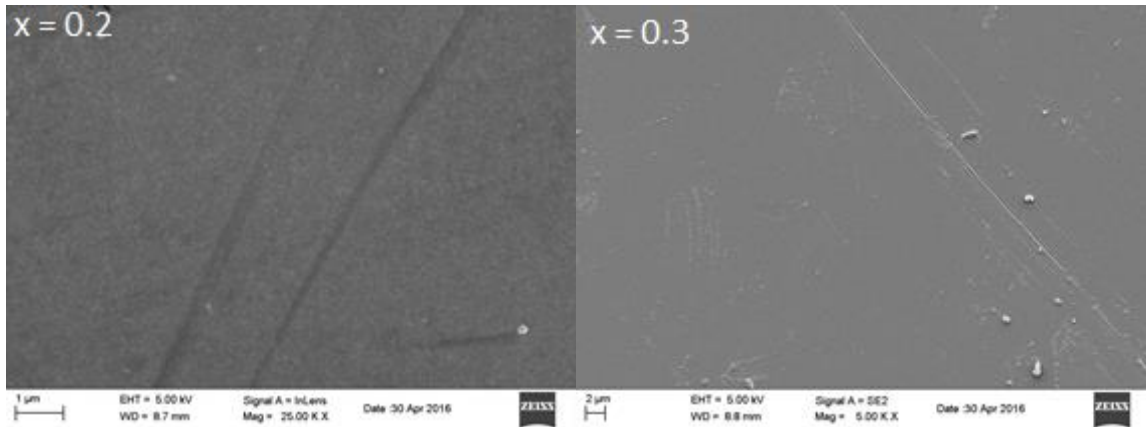


Figure 3.2: FE-SEM images shows very smooth surfaces of the ZITO thin films.

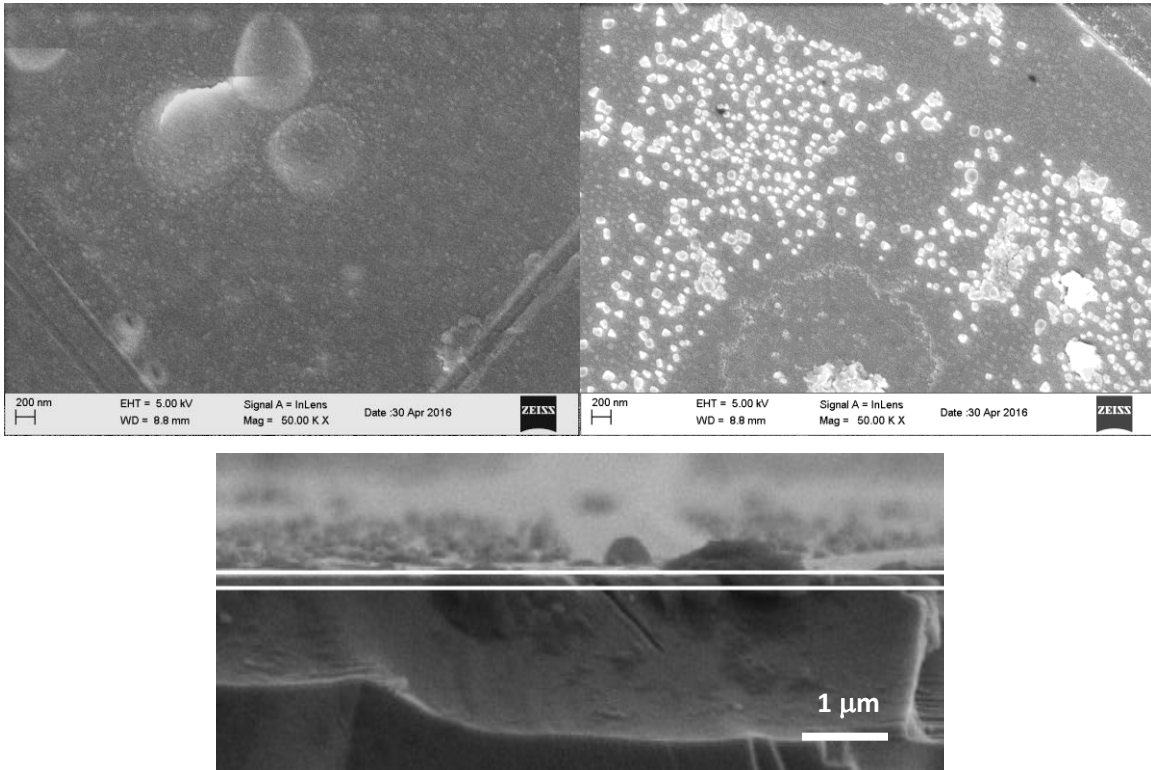


Figure 3.3: FE-SEM images at higher magnification showing surfaces of the ZITO ($x = 0.3$) thin films. The cross-sectional image is also given, which shows the thickness to be ~ 95 nm.

3.3 Optical properties of ZITO thin films

The UV-visible transmittance curve for the ZITO thin films (with different values of x) grown by the spin coating process is shown in **Figure 3.4**. Although the XRD patterns did not reveal any difference between the films of different composition, there was small but noticeable difference in their optical transmittance curves. The film shows very high transmittance $> 90\%$ in the range of 350 – 1400 nm, irrespective of their composition. The high transmittance shows the suitability of the material for developing the transparent TFTs.

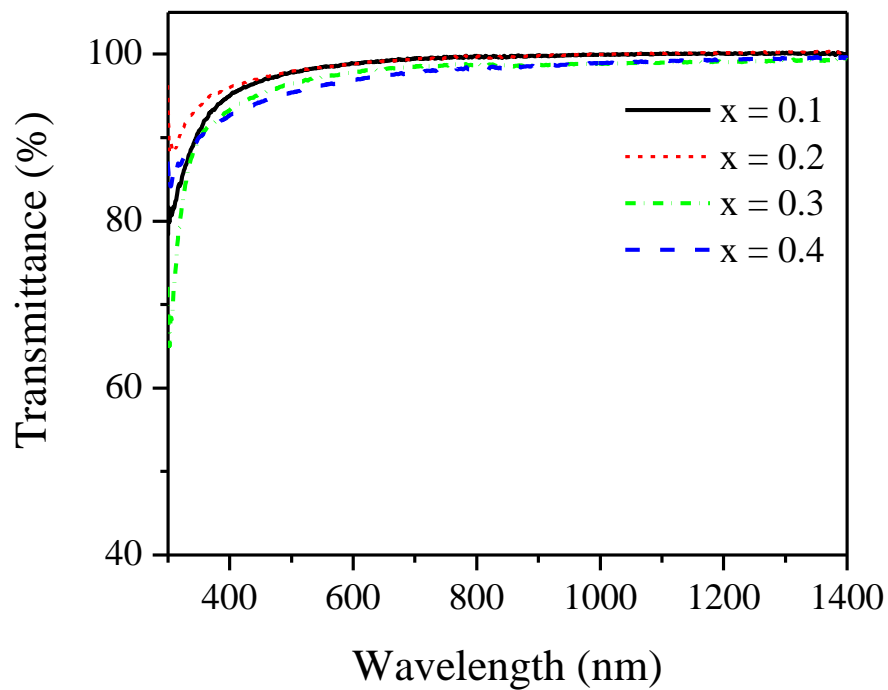


Figure 3.4: Transmittance (%) spectrum of the ZITO thin films with $x = 0.1$ to 0.4

Quantitative evaluation of the band gap was carried out from the Tauc plots, i.e., from the variation of $(\alpha h\nu)^{1/2}$ vs. $h\nu$ and by extrapolating the linear region. The plot of $(\alpha h\nu)^{1/2}$ vs. $h\nu$ is shown in **Figure 3.5**. Accordingly, we have estimated the band gap. The band gap of the prepared samples with $x = 0.1$ and 0.3 was found to be 2.72 and 3.35 eV, which is similar to the values reported in literature.

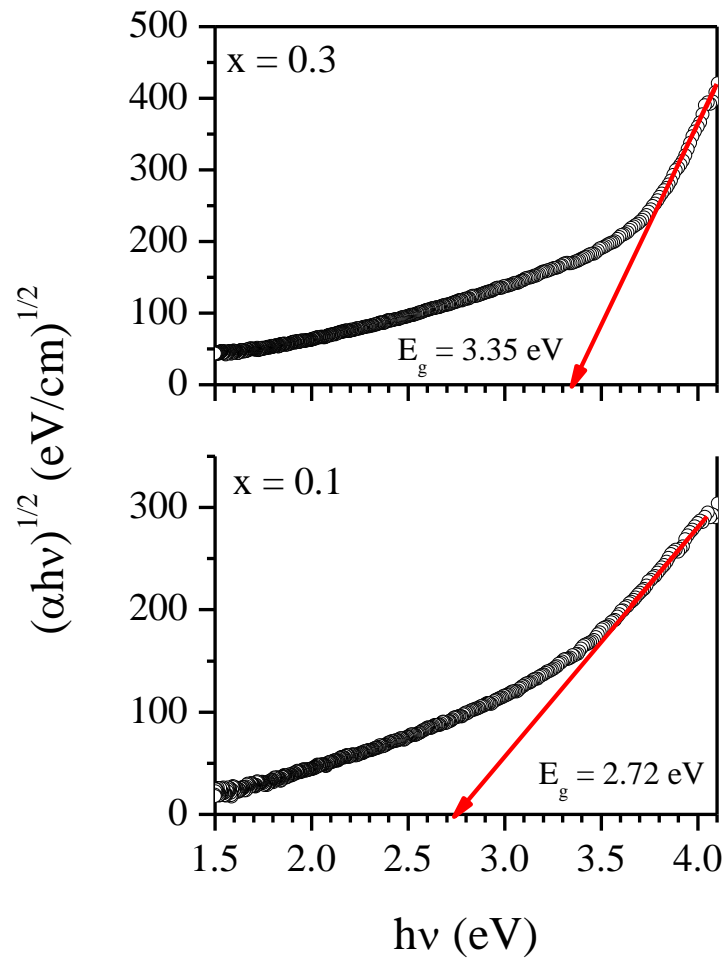


Figure 3.5: Plot of $(\alpha hv)^{1/2}$ vs $h\nu$ for the ZITO thin films with $x = 0.1$ and 0.3 .

CHAPTER 4

SUMMARY AND FUTURE SCOPE

ZITO ($\text{In}_{2-2x}\text{Zn}_x\text{Sn}_x\text{O}_{3+\delta}$, with $x = 0.1-0.4$) thin films were grown by the spin coating process. Since the control of process parameters is very easy, this technique has been used in deposition of thin films of many technologically important materials. The thickness of the films made by the spin coating method depends mainly on the rotation speed, time of spinning, viscosity and liquid concentration. Under the given experimental condition, the thickness of the obtained film was about 95 nm. The properties of the films were investigated using a variety of techniques such as XRD, FE-SEM, and UV-visible spectroscopy.

The prepared ZITO thin films were found to be amorphous in nature irrespective of their composition. An examination of the film revealed that the film surface is covered with very fine nano-sized particles. The films with $x = 0.3$ exhibited very high transmission better than 90% in the visible portion of the electromagnetic spectrum, with a band gap of about 3.35 eV. The results of this work indicate that amorphous ZITO thin films can be prepared successfully by the simple deposition technique such as spin coating. It would be interesting to study temperature stability of the amorphous phase of the material (which is crucial to efficient TFTs). Besides, further work should include study of the electrical properties fabrication of devices.

References

- 1 “Thin Films: Raw Materials, Technology and Applications,” BCC Research Report code SMC057A (2005).
- 2 Yue Kuo, “Thin Film Transistor Technology – Past, Present and Future,” The Electrochemical Society Interface Spring (2013).
- 3 Jang-Yeon Kwon, Do-Joong Lee and Ki-Bum Kim, “Review Paper: Transparent Amorphous Oxide Semiconductor Thin Film Transistor,” *Electronic Materials Letters* 7, 1 (2011).
- 4 E. Fortunato, P. Barquinha, and R. Martins, “Oxide Semiconductor Thin-Film Transistors: A Review of Recent Advances,” *Advanced Materials* 24, 2945 (2012).
- 5 Jun Liu, D. Bruce Buchholz, Robert P. H. Chang, Antonio Facchetti, and Tobin J. Marks, “High-Performance Flexible Transparent Thin-Film Transistors Using a Hybrid Gate Dielectric and an Amorphous Zinc Indium Tin Oxide Channel,” *Advanced Materials* 22, 2333 (2010).
- 6 Myung-Gil Kim, Hyun Sung Kim, Young-Geun Ha, Jiaqing He, Mercuri G. Kanatzidis, Antonio Facchetti and Tobin J. Marks, “High-Performance Solution-Processed Amorphous Zinc-Indium-Tin Oxide Thin-Film Transistors,” *Journal of American Chemical Society* 132, 10352 (2010).
- 7 K. J. Chen, F. Y. Hung, S. J. Chang, S. J. Young, Z. S. Hu and S. P. Chang, “An investigation of the microstructure, optical and electrical properties of ZITO thin film using the sol–gel method,” *J Sol-Gel Sci Technol* 54, 347 (2010).
- 8 D. Bruce Buchholz, Jun Liu, Tobin J. Marks, Ming Zhang and Robert P. H. Chang, “Control and Characterization of the Structural, Electrical, and Optical Properties of Amorphous Zinc-Indium-Tin Oxide Thin Films,” *Applied materials & interfaces* 1(10), 2147 (2009).
- 9 Y. Natsume and H. SakataU, “Zinc oxide films prepared by sol-gel spin-coating,” *Thin Solid Films* 372, 30 (2000).
- 10 Hoffman, B. J. Norris, and J. F. Wager, “ZnO-based transparent thin-film transistors,”

- Applied Physics Letters 82, 733 (2003).
- 11 P. F. Carcia, R. S. McLean, M. H. Reily, and G. Nunes, "Transparent ZnO thin-film transistor fabricated by RF magnetron sputtering," *Applied Physics Letters* 82, 1117 (2003).
 - 12 B. J. Norris, J. Anderson, J. F. Wager, and D. A. Keszler, "Spin-coated zinc oxide transparent transistors," *Journal of Physics D: Applied Physics* 36, 105 (2003).
 - 13 R. E. Presley, C. L. Munsee, C.H. Park, D. Hong, J. F. Wager, and D. A. Keszler, "Tin oxide transparent thin-film transistors," *Journal of Physics D: Applied Physics* 37, 2810 (2004).
 - 14 R. B. H Tahar, T. Ban, Y. Ohya, and Y. Takahashi, "Tin doped indium oxide thin films: Electrical properties," *Journal of Applied Physics* 83, 2631 (1998).
 - 15 J. H. Jeon, Y. H. Hwang, B. S. Bae, H. L. Kwon, and H. J. Kang, "Addition of aluminum to solution processed conductive indium tin oxide thin film for an oxide thin film transistor," *Applied Physics Letters* 96, 212109 (2010).
 - 16 H. Q. Chiang, J. F. Wager, R. L. Hoffman, J. Jeong, and D. A. Keszler, "High mobility transparent thin-film transistors with amorphous zinc tin oxide channel layer," *Applied Physics Letters* 86, 013503 (2005).
 - 17 D. Hong and J. F. Wager, "Passivation of zinc-tin-oxide thin-film transistors," *Journal of Vacuum Science & Technology B* 23, L26 (2005).
 - 18 R. L. Hoffman, "Effects of channel stoichiometry and processing temperature on the electrical characteristics of zinc tin oxide thin-film transistors," *Solid State Electronics* 50, 784 (2006).
 - 19 Seok-Jun Seo, Chaun Gi Choi, Young Hwan Hwang and Byeong-Soo Bae, "High performance solution-processed amorphous zinc tin oxide thin film transistor," *Journal of Physics D: Applied Physics* 42, 035106 (2009).
 - 20 N. L. Dehuff, E. S. Kettenring, D. Hong, H. Q. Chiang and J. F. Wager, "Transparent thin-film transistors with zinc indium oxide channel layer," *Journal of Applied Physics* 97, 064505 (2005).

- 21 P. Barquinha, A. Pimentel, A. Marques, L. Pereira, R. Martins, and E. Fortunato, "Influence of the semiconductor thickness on the electrical properties of transparent TFTs based on indium zinc oxide," *J. Non-Crys. Sol.* 352, 1749 (2006).
- 22 Ye Wang, Xiao Wei Sun, Gregory Kia Liang Goh, Hilmi Volkan Demir, and Hong Yu Yu, "Influence of Channel Layer Thickness on the Electrical Performances of Inkjet-Printed In-Ga-Zn Oxide Thin-Film Transistors," *IEEE Transactions On Electron Devices* 58, 2 (2011).
- 23 K. Nomura, H. Ohta, K. Ueda, T. Kamiya, M. Hirano, and H. Hosono, "Thin film transistor fabricated in single-crystalline transparent oxide semiconductor," *Science* 300, 1269 (2003).
- 24 Cathleen A. Hoel, Thomas O. Mason, Jean-Francois Gaillard, and Kenneth R. Poeppelmeier, "Transparent Conducting Oxides in the ZnO-In₂O₃-SnO₂ System," *Chemistry of Materials* 22, 3569 (2010).
- 25 Steven P. Harvey, Kenneth R. Poeppelmeier and Thomas O. Mason, "Subsolidus Phase Relationships in the ZnO-In₂O₃-SnO₂ System," *Journal of the American Ceramic Society* 91, 3683 (2008).
- 26 D.B. Buchholz, D.E. Proffit, M.D. Wisser, T.O. Mason, R.P.H. Chang. "Electrical and band-gap properties of amorphous zinc-indium-tin oxide thin films," *Progress in Natural Science: Materials International* 22(1), 1-6 (2012).
- 27 Clewa W. Ow-Yang, Hyo-young Yeom and David C. Paine, "Fabrication of transparent conducting amorphous Zn-Sn-In-O thin films by direct current magnetron sputtering," *Thin Solid Films* 516 3105 (2008).
- 28 M. Zhang, D.B. Buchholz, S.J. Xie and R.P.H. Chang, "Twinned domains in epitaxial ZnO/SnO₂-cosubstituted In₂O₃ thin films," *Journal of Crystal Growth* 308, 376 (2007).
- 29 M. S. Grover, P. A. Hersh, H. Q. Chiang, E. S. Kettenring, J. F. Wager and D. A. Keszler, "Thin-film transistors with transparent amorphous zinc indium tin oxide channel layer," *Journal of Physics D: Applied Physics* 40, 1335 (2007).
- 30 Min Ki Ryu, Shinhyuk Yang, Sang-Hee Ko Park, Chi-Sun Hwang, and Jae Kyeong Jeong, "Impact of Sn/Zn ratio on the gate bias and temperature-induced instability of Zn-In-Sn-O

- thin film transistors,” *Applied Physics Letters* 95, 173508 (2009).
- 31 Paz Carreras, Aldrin Antony, Fredy Rojas, Joan Bertomeu, “Electrical and optical properties of Zn–In–Sn–O transparent conducting thin films,” *Thin Solid Films* 520, 1223 (2011).
 - 32 D.B. Buchholz, D.E. Proffit, M.D. Wisser, T.O. Mason, R.P.H. Chang, “Electrical and Band-Gap Properties of Amorphous Zinc–Indium–Tin Oxide Thin Films,” 22(1), 1 (2012).
 - 33 A. Marsal, P. Carreras, J. Puigdollers, C. Voz, S. Galindo, R. Alcubilla, J. Bertomeu, A. Antony, “Compositional influence on the electrical performance of zinc indium tin oxide transparent thin-film transistors,” *Thin Solid Films* 555, 107 (2014).
 - 34 C.Brinker, C.Scherer, “The Physics and Chemistry of Sol-Gel Processing,” Academic Press, San Diego (1990).
 - 35 Niranjana Sahu, B. Parija and S Panigrahi, “Fundamental understanding and modeling of spin coating process: A review,” *Indian J. Phys.* 83, 493 (2009).
 - 36 Sohrab Ahmadi Kandjani, Soghra Mirershadi and Arash Nikniaz, “Inorganic–Organic Perovskite Solar Cells” (2014).
 - 37 Myung-Gil Kim, Hyun Sung Kim, Young-Geun Ha, Jiaqing He, Mercuri G. Kanatzidis, Antonio Facchetti and Tobin J. Marks, “High-Performance Solution-Processed Amorphous Zinc-Indium-Tin Oxide Thin-Film Transistors,” *Journal of American Chemical Society* 132, 10352 (2010).
 - 38 I. M. Watt, “The principles and practice of electron microscopy”, Cambridge University Press, Cambridge (1983).
 - 49 P. J. Goodhew, J. Humphreys and R. Beanland, “Electron Microscopy and Analysis”, Taylor Francis, London (2000).
 - 40 K. S. Birdi, “Scanning Probe Microscopes: Applications in Science and Technology”, CRC Press, Boca Raton (2003).
 - 41 E. Meyer, H. J. Hug and R. Bennewitz, “Scanning Probe Microscopy: The Lab on a Tip”, Springer- Verlag Berlin (2004).

- 42 S. Morita, R. Wiesendanger and E. Meyer, “Noncontact Atomic Force Microscopy”, Springer: Berlin (2002).
- 43 A. Mehta, “UV-Vis Spectroscopy- Limitations and Deviations of Beer- Lambert Law”, Analytical Chemistry (2012).
- 44 P. Misra and M. A. Dubinskii, “Ultraviolet Spectroscopy and Uv- Lasers”, New York, Marcel Dekker (2002).
- 45 B. W. Kempshall, L. A. Giannuzzi, B. I. Prenitzer, F. A. Stevie and S. X. Da, “Comparative Evaluation of Protective Coatings and Focused Ion Beam Chemical Vapor Deposition Processes”, J. Vacuum Sci. Technol. B 20, 286 (2002).
- 46 Zelaya-Angel, J.J. Alvarado-Gil, R. Lozada-Morales, H. Vargas and A. Ferreira da Silva, “Band-Gap Shift in CdS Semiconductor by Photo acoustic Spectroscopy: Evidence of a Cubic to Hexagonal Lattice Transition”, Appl. Phys. Lett. 64, 291 (1994).
- 47 M. Rusu, A. Rumberg, S. Schuler, S. Nishiwaki, R. Wurz, S.M. Babu, M. Dzedzina, C. Kelch, S. Siebentritt, R. Klenk, Th. Schedel-Niedrig and M.Ch. Lux-Steiner, “Optimisation of the CBD CdS Deposition Parameters for ZnO/CdS/CuGaSe Solar Cells”, J. Phys. Chem. Solids 64, 1849 (2003).